Fault tolerance analysis for a class of reconfigurable aerial hexarotor vehicles

Claudio D. Pose, Juan I. Giribet, *Senior Member, IEEE,* and Ignacio Mas, *Senior Member, IEEE*

***Abstract*—Several works have addressed the issue of fault tolerance in multirotors in case of a rotor total failure, particularly their ability to keep full independent control of attitude and altitude. It has been proven that to achieve this, a minimum of six rotors is needed.**

In this work, the performance of several standard and non-standard hexarotor structures is analyzed, both for a nominal case (without failure) and in the case where one of the actuators is under failure (incapability to exert thrust). The performance is shown in terms of maximum rotational torque and vertical force that the vehicle can exert.

The main contribution of this work is the proposal and analysis of converting these vehicles into reconfigurable ones through the addition of a minimum number of servomotors, to deal with failures and to greatly improve the maneuverability under these conditions, in order to identify the reconfigurable structure with the best performance. An experimental demonstration in an outdoor environment is shown for the proposed reconfigurable structure with best performance in case of a full rotor failure.

***Index Terms*—Fault tolerance, UAV, reconfigurable, control allocation, hexarotor.**

I. Introduction

MULTIROTOR aerial vehicles have become very popular in recent years, due to the availability of the electronic systems required for operation and the reduction of their cost and weight. Simplicity and cost-effectiveness led to an increasing number of applications in diverse fields, such as agriculture, surveillance, and photography, among others. Fault tolerance has been addressed in the literature as a matter of high importance, in particular for multirotor vehicles, see for instance [1], [2], [3], [4], [5], [6], [7], [8], [9], [10], and references therein.

In [11], the capability of compensating for a rotor failure without losing the ability to exert torques in all directions, and therefore keeping full attitude control in case of failure, is studied. For this, at least six rotors are needed, and the proposed solution is to tilt the rotors inwards with respect to the vertical axis of the vehicle. Experimental results for the proposed solution can be found in [12], where the vehicle takes off, performs different maneuvers and lands successfully with one motor in total failure, maintaining full attitude and altitude control. While the system proved to work correctly, there was a direction that, when exerted torque in, performed noticeably worse with respect to the rest. In [13], a detailed analysis is made with respect to the optimal orientations of the rotors in a hexarotor, in order to achieve full tolerant attitude control. Still, the maximum torque achievable in some directions may be too small, with the consequent degradation of vehicle maneuverability.

Other known solutions for fault tolerance in a hexarotor vehicle are analyzed in [14], where changing the spinning direction of unidirectional rotors allowed for fault tolerance for four of the six cases of failure, and in [15], where the use of bidirectional actuators is proposed. Also, octorotor structures have been proposed for fault tolerance as they rely on actuator redundancy to solve this issue, at the cost of a bigger structure or a loss of thrust efficiency (this last one in coaxial models). Several structures have been analyzed over the years, using different techniques to evaluate the limitations of fault tolerance in this kind of vehicles [16].

This article analyzes several hexarotor structures and their fault tolerant capabilities, which have been previously treated in the literature, and focuses on a proposed modification to convert these structures into reconfigurable ones, in order to significantly improve the maneuverability in case of a total failure in one rotor. The main interest is to identify which of the reconfigurable structures presents the best maneuverability in case of a failure in any of its rotors. The manuscript is organized as follows. Section II presents the vehicles to be analyzed and generalities regarding their mechanics. Section III introduces the metrics used to compare the different structures, and Section IV adds insight into the design considerations for tilted-rotor vehicles. Section V and VI analyze the metrics for the considered vehicles in a nominal case and in case of a single rotor failure, respectively. Finally, Section VII presents the proposed modifications to transform the vehicles into reconfigurable ones, and show the improvements in the metrics, while Section VIII shows an experimental proof of concept for the vehicle with best performance.

II. Interest in hexarotor vehicles

Throughout this work, a failure in a rotor will be considered as the incapability of that rotor to exert any thrust, and a vehicle will we considered fault tolerant if it is able to overcome the failure while maintaining full attitude and altitude control (4DOF - four degrees of freedom). While there exist many solutions that deal with this kind of failure by giving up control over one or more degrees of freedom in case of a

Claudio D. Pose, Juan I. Giribet and Ignacio Mas are with the Laboratorio de Automática y Robótica (LAR) - Facultad de Ingeniería, Universidad de Buenos Aires, Buenos Aires, Argentina. [cldpose, jgiribet, imas]@fi.uba.ar

Juan I. Giribet is with the Instituto Argentino de Matemática - CONICET, Buenos Aires, Argentina.

Ignacio Mas is with CONICET and Instituto Tecnológico de Buenos Aires (ITBA), Buenos Aires, Argentina.

failure (being the heading angle control usually the first one to be relinquished [17]), there are several applications where the vehicles cannot afford to implement this solution.

As six is the minimum number of rotors needed to achieve fault tolerance, this work will put the focus on hexarotor vehicles, as it is desired to achieve fault tolerance with the minimum possible number of actuators. There exist several designs for hexarotor vehicles, that deal not only with fault tolerance, as some of them aim to improve maneuverability, others to decrease their mechanical complexity, an others to achieve full independent position and attitude control.

In this work, six different models of hexarotors are analyzed:

- Standard (**STD**): This vehicle has its six rotors distributed in a co-planar way, placed in the vertices of a regular hexagon, all of them pointing in the same direction, perpendicular to the plane that contains them, as shown in Fig. 1 (left). Consecutive rotors have alternate spinning direction, beginning with rotor 1 spinning counterclockwise (CCW) or in positive (P) direction w.r.t. the Z axis, rotor 2 spinning clockwise (CW) or in negative (N) direction, and so on, which is generally known as a PNPNPN hexarotor. This vehicle is able to control independently its attitude and altitude. Position control is only achievable through attitude maneuvers.
- Alternative spinning disposition (**PPNN**): The distribution of rotors in this vehicle is the same as the **STD**. In this case, rotors 1, 2 and 5 spin CCW, and rotors 3, 4 and 6 spin CW, which is generally known as a PPNNPN hexarotor. This design proved to be fault tolerant in case of rotor failures in rotors 1 to 4, but not for rotors 5 or 6 [14].
- Coaxial (**COAX**): In this case, the vehicle has only three arms, each of which has two rotors mounted coaxially, with their axes all pointing in the same direction, as shown in Fig. 1 (right). The thrust force is generated in the same sense. Rotors 1 to 3 are the top ones and spin CCW, and rotors 4 to 6 are the bottom ones and spin CW. A downside to this design is that, as the bottom rotor receives accelerated air from the top one, its thrust efficiency is degraded [18].
- Symmetric inwards-tilted (**INW**): The position of the rotors is the same as described for the **STD** vehicle (Fig. 1 (left)), but in this case all the rotors are tilted inwards at the same angle γ as defined in Fig. 2 (left). The spinning direction of the rotors is PNPNPN. This vehicle has been proven to be fault tolerant in case of a failure in any of its rotors [11], [12].
- Symmetric side-tilted (**SIDE**): Again, the position of the rotors is the same as the **STD** vehicle, but with all the rotors tilted sideways at the same angle δ as defined in Fig. 2 (right). As a rotor is exerting torque in the Z axis due to the spinning propeller, the angle δ is defined positive if the rotor is tilted in such a way that this torque is increased. As the Z axis is the one in which it is most difficult to exert torque, this design is intended to improve the maneuverability in that axis in the nominal case [13].
- Symmetric inwards- and side-tilted (**DUAL**): A combination of the last two vehicles, it has been shown that side-tilting the rotors may also increase the maneuverability of the inwards-tilted vehicle in case of a failure [13].

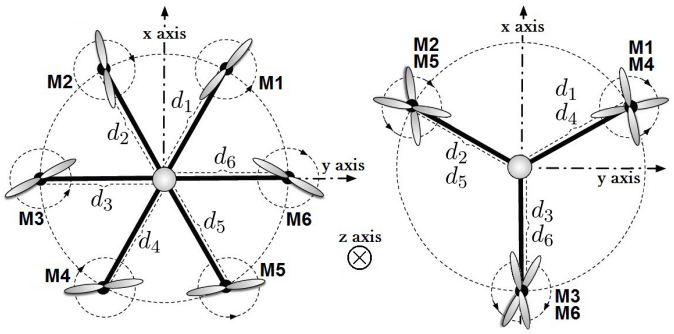

Fig. 1. Co-planar (left) and coaxial (right) hexarotor distributions.

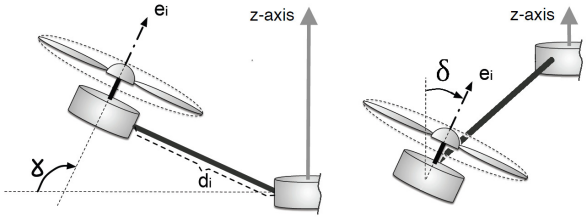

Fig. 2. Inwards tilting angle γ (towards the center of the vehicle) and side-tilting angle δ (over the arm's axis).

The last three vehicles mentioned are also capable to independently control position and attitude in a nominal state.

For each vehicle, the body axes and rotor numbering will be those presented in Fig. 1.

A. Feasible torque set

In a normal state of operation, each unidirectional rotor-propeller set produces a force $\tilde{f}_i \in [0, F_M]$, being F_M the maximum force at top speed. In practice, each motor's speed is commanded through a Pulse Width Modulated (PWM) signal u_i, which takes a value between 0 and 100%. Near the nominal operating point, a linear relation between the PWM signal and the exerted force is assumed, with $\tilde{f}_i = k_f u_i$. It is also considered that each motor exerts a torque on its spinning axis, $m_i = \pm k_t u_i$, where the sign depends on the spinning direction, which may also be expressed as $m_i = \pm(k_t/k_f)\tilde{f}_i$. The $k_f, k_t > 0$ constants are usually established experimentally.

The total vehicle force $f \in \mathbb{R}^3$ (with $f = (f_x, f_y, f_z)^T$) and torque $q \in \mathbb{R}^3$ in the body frame coordinates satisfies:

$$f = k_f E u, \qquad q = (k_t E J + k_f H)\, u \tag{1}$$

$$E = [e_i]_{i=1,n}, \qquad H = [d_i \times e_i]_{i=1,n}, \tag{2}$$

Here, the location of the center of mass of the i–th motor is given by the column vector $d_i \in \mathbb{R}^3$, and the direction of the corresponding force is given by the column vector $e_i \in \mathbb{R}^3$. Both vectors are represented in body frame coordinates. J is a diagonal matrix with diagonal entries $j_{ii} = \pm 1$, for $i = 1, ..., n$, depending on the spinning direction of each rotor.

Given an arbitrary torque $q \in \mathbb{R}^3$ and a (nonnegative) ascent force $f_z \geq 0$, by equation (1) it follows that there is a linear relation between the desired torque and force $(q^T, f_z)^T$ and the PWM signals $u \in \mathbb{R}^n$. Let $A \in \mathbb{R}^{4\times n}$ be such matrix:

$$\begin{bmatrix} q \\ f_z \end{bmatrix} = Au$$

Since u belongs to a hypercube $\mathcal{U}$, it follows that the reachable torque-force set is a convex polytope $\mathcal{C} \subseteq \mathbb{R}^4$. Assuming that the rotor positions are not modified, if one motor fails (i.e., $u_i = 0$), the corresponding polytope is contained in $\mathcal{C}$.

In practice however, the control allocation problem is usually solved by means of the Moore-Penrose pseudoinverse of A, denoted $A^\dagger$. More precisely, given the desired torque and thrust $z = (q^T, f_z)^T \in \mathbb{R}^4$, the PWM signals are calculated as $u = A^\dagger z$. Recall that Moore-Penrose pseudoinverse satisfies $AA^\dagger = P_{R(A)}$ and $A^\dagger A = P_{N(A)^\perp}$, where $N(A)$ and $R(A)$ are the kernel and range of A respectively, and $P_{\mathcal{S}}$ denotes the orthogonal projection onto the subspace $\mathcal{S}$.

Since the PWM must lie in the hypercube $\mathcal{U}$, in this case the reachable torque-thrust set is the subset of $\mathcal{C}$, given by:

$$\mathcal{R} = \{z \in \mathcal{C} : A^\dagger z \in \mathcal{U}\}. \tag{3}$$

The reason why the Moore-Penrose is commonly used to solve the control allocation problem is because it provides the minimum energy-norm PWM signals that give the desired torque and thrust. The next lemma gives a simpler characterization of the set of reachable torque-thrust.

Lemma 2.1: Let $A \in \mathbb{R}^{4\times n}$ be a full-rank matrix, and define the set R as in equation (3). Then $\mathcal{R} = A(R(A^T) \cap \mathcal{U})$.

Proof. First, recall that $R(A^\dagger) = N(A)^\perp = R(A^T)$. Now, suppose that $z \in \mathcal{R}$, then $A^\dagger z \in \mathcal{U} \cap R(A^T)$; since A is a full-rank matrix, it follows that $z = A(A^\dagger z)$, then $z \in A(\mathcal{U} \cap R(A^T))$. On the other hand, suppose that $z \in A(\mathcal{U} \cap R(A^T)) \subseteq \mathcal{C}$ and let $u \in \mathcal{U} \cap R(A^T)$ such that $Au = z$. Since $A \in R(A^T) = N(A)^\perp$, it follows that $u = A^\dagger Au \in \mathcal{U}$. Then $z = Au \in \mathcal{R}$. □

This lemma shows that $\mathcal{R} = \mathcal{C}$ if and only if $\mathcal{U} \subseteq R(A^T)$, in this case the set of reachable torque-sets computed with the Moore-Penrose psudoinverse is the whole set $\mathcal{C}$. But this condition usually does not hold, so a more restrictive set of torque-thrust is achievable. However, using the Moore-Penrose pseudoinverse to calculate the PWM signals reduces the computational burden considerably.

In a hovering condition, the thrust compensates the weight of the vehicle ($-mg$). Therefore, to study the reachable torque set under hovering condition, we need to restrict the analysis to the linear manifold $\mathcal{L} = \{(q^T, -mg)^T \in \mathbb{R}^4, q \in \mathbb{R}^3\}$. More precisely, we are interested in characterizing the set

$$\mathcal{U}' = A^\dagger(\mathcal{L} \cap \mathcal{C}) = A^\dagger(\mathcal{L}) \cap \mathcal{U}.$$

which is the set of minimum-energy norm propeller PWM signals ensuring hovering condition.

B. Vehicle's characteristics

To compare the vehicles, it is assumed that all of them have similar characteristics, and that they resemble commercially available vehicles. As reference, a DJI F550 hexarotor main structure is used for all vehicles, which is designed for coplanar distributions but may be adapted for coaxial designs, and presents a rotor-to-rotor distance of $0.55\,\mathrm{m}$. The actuator sets used are standard kits from DJI, composed of 920KV, 2212-size rotors, 9443 plastic self-tightening propellers and E300 electronic speed controllers, which on a 4S LiPo battery ($14.8\,\mathrm{V}$) can exert up to $1\,\mathrm{kg}$ of force. The $\tilde{k}_t$ factor of this set has been experimentally found to be 0.05, (usually this value ranges around [0.02-0.1], depending on the propeller size and material). In general, in commercial systems, the actuator groups are selected so that the maximum total thrust exerted doubles the weight of the vehicle. This is because in practice, generally, the **STD** structure is used, and this selection of actuators allows for the maximum maneuverability of the vehicle, while also considering a possible payload of $0.5\,\mathrm{kg}$ or less. Then, it is a reasonable consideration that the vehicles weight $3\,\mathrm{kg}$. A summary of the features of the vehicles, along with a range of typical values, are shown in Table I.

TABLE I
HEXAROTOR TYPICAL FEATURES

———	Selected	Typical	Unit
Weight	3	2.5 - 3.5	kg
Max. Thrust per motor	1	0.8 - 1.5	kg
Inertia moment X,Y	0.004	0.002 - 0.01	kgm^2
Inertia moment Z	0.01	0.005 - 0.03	kgm^2
k_f	0.0125	0.00625 - 0.015	kg/%
$\tilde{k}_t$	0.05	0.02 - 0.1	-
Rotor to rotor distance	0.55	0.4 - 0.7	m
LiPo battery voltage	14.8	11.1 - 22.2	V

III. PERFORMANCE METRICS

To analyze and compare the different vehicles, several performance markers that define the maneuverability of a vehicle are taken into account:

- Maximum torque achievable in any direction (q_{max}): Considering the vehicle is in hovering state, $q_{max} \geq 0$ is the modulus of the maximum torque that can be exerted in any direction. If $\|q\| \leq q_{max}$ then $(q^T, -mg)^T \in \mathcal{L} \cap \mathcal{C}$. Usually the torque exertion in the *Z* axis is more restrictive.
- Maximum torque achievable in the *XY* plane ($q_{max}XY$): Again considering the hovering state, $q_{max}XY > 0$ is the modulus of the maximum torque that may be exerted considering the *XY* plane. In a standard flight mission, maneuvers over these axes are more common than those on the *Z* axis, as they are needed for position control.
- Maximum vertical force (f_z max): This is the vehicle's maximum vertical climbing force, that is, the maximum force exceeding the vehicle's weight that can be exerted.
- Current consumption (Cons.): The consumption of the vehicle provides an estimate of the energy needed to maintain the vehicle in hovering state, and is related to the maximum flight time for a given vehicle. The values will be analyzed based on measurements on real actuators.

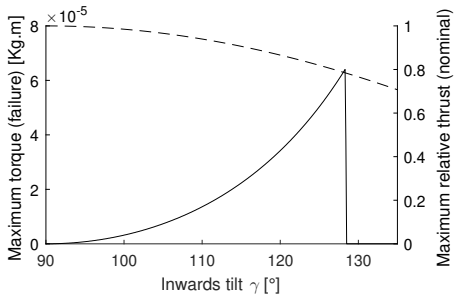

Fig. 3. q_{max} in a failure case (continuous line, left axis) and maximum relative thrust in the nominal case w.r.t. the **STD** vehicle (dashed line, right axis), for a variable inwards tilt angle γ in a **INW** vehicle.

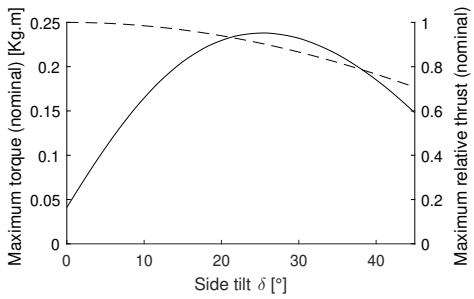

Fig. 4. q_{max} (continuous line, left axis) and maximum relative thrust w.r.t. the **STD** vehicle (dashed line, right axis), both in the nominal case, for a variable side tilt angle δ in a **SIDE** vehicle.

To construct the attainable torque set for each of the structures considered, a numerical analysis is carried out. As Algorithm 1 shows, for every vehicle considered, the attainable maximum torque in every direction $\hat{q}$ is evaluated (with a granularity in θ and α of 0.5 degrees). For each direction, a torque is considered achievable if the solution of the pseudoinverse is feasible, that is, if $u \in \mathcal{U}'$.

Algorithm 1 Attainable Torque Set search

Require: rank(A_i)==4, q_{init}, $limit$
  for $\theta \in [0, 2\pi)$, $\alpha \in [0, \pi)$
    $\hat{\mathbf{q}} = [sin(\alpha)cos(\theta), sin(\alpha)sin(\theta), cos(\alpha)]$
    $q_{mod} = q_{init}$, $step = q_{init}/2$
    while $step > limit$
      $u = A^{\dagger}[q_{mod}\hat{\mathbf{q}}, -mg]^T$
      if $any(u_i) < 0$ or $any(u_i) > 100\%$
        then $q_{mod} -= step$ **else** $q_{mod} += step$
      $step = step/2$

IV. Design considerations

While the **STD**, **PPNN**, and **COAX** vehicles are completely defined by the aforementioned rotors' positions and vehicle's characteristics, the **INW**, **SIDE**, and **DUAL** models depend on design considerations to choose the inwards and sideways tilting angles. For the **COAX** vehicle, the loss of efficiency due to the shared airflow of the coaxial rotors is taken into account.

The **INW** model, as proposed in [11], improves the q_{max} in a failure case as the tilt angle increases, however, this leads to a loss of maximum vertical thrust, both in the nominal and in the failure case, which also leads to a higher working point of the actuators, nearer saturation. In Fig. 3, the q_{max} in a failure case and the maximum relative thrust in the nominal case (considering $\gamma = 90^o$ as reference for the latter) are shown, for a variable inwards tilt angle between 90^o and 135^o (the same for all the rotors). It should be noted that increasing the tilt angle indiscriminately does not guarantee an increasing value of q_{max}, as the loss of vertical thrust leads to a saturation of one of the rotors at around $\gamma = 128^o$. For this work, it is considered that the maximum allowable vertical thrust loss in the nominal case is 10% with respect to the **STD** case, which leads to an inwards tilt angle of $\gamma = 115^o$.

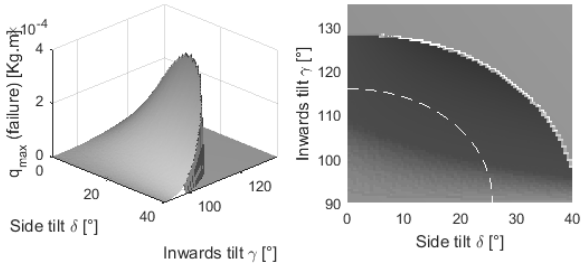

Fig. 5. Left figure shows q_{max} in the failure case, for a variable side tilt angle δ and inwards tilt angle γ in a **DUAL** vehicle. Right figure presents a top view, with a dashed white line showing the dual tilting limit for a thrust loss of 10% in the nominal case.

For the **SIDE** vehicle, the purpose of tilting the rotors sideways is to increase the maximum achievable torque in the Z axis in the nominal case, which in turn also increases q_{max}. In Fig. 4 it is shown both the q_{max} and the maximum relative thrust in a nominal case, for a variable side tilt angle between 0^o and 45^o (the same for all the rotors). It should be noted that there is, in a sense, an optimal point at $\delta = 25^o$, where q_{max} is maximized, and where the vertical thrust loss is 10%, which will be the chosen configuration to analyze.

Finally, for the **DUAL** vehicle, tilting the rotors increases the q_{max} in a failure case, similarly as in the **INW** vehicle. However, it should be mentioned that the improvement in the q_{max} due to the inwards tilt is not the same to that due to the sideways tilt. A similar analysis to the one of the **INW** is shown in Fig. 5, where q_{max} is shown for a failure case, and it is found that, for a maximum 10% thrust loss, the optimal tilt angles are $\gamma = 110^o$ and $\delta = 16^o$.

V. Nominal operation

To provide a compact and understandable comparison of the different vehicles, Table II presents the magnitudes of the performance markers in nominal conditions (without failure) while hovering, for all the vehicles, where the best features are marked in dark gray, and the second best in light gray.

As expected, in the nominal case, the **SIDE** vehicle shows the best performance with respect to q_{max}. Generally, the Z axis is the one in which it is most difficult to exert torque in, then, tilting the rotors sideways to increase the torque in that axis greatly improves q_{max}. In terms of this performance

TABLE II
NOMINAL CHARACTERISTICS OF THE VEHICLES

Vehicle	q_{max} [kg m]	q_{max} XY [kg m]	f_z max [kg]	Cons. [A]
STD	0.0411	0.412	3	27.1
PPNN	0.0240	0.299	3	27.1
COAX	0.0287	0.289	2.1	27.1
INW 115^o	0.0334	0.335	2.44	31.2
SIDE 25^o	0.2380	0.327	2.44	31.8
DUAL 110^o+ 16^o	0.1850	0.328	2.44	31.4

TABLE III
STANDARD DEVIATION OF TORQUES IN A NOMINAL CASE

Type of flight	σ_{xy} [kg m]	σ_z [kg m]
Near hovering	0.016	0.00171
Average	0.0223	0.003
Aggresive	0.0315	0.00367

marker, it is followed by the **DUAL** design, whose side tilt component results in the same kind of improvement.

Regarding the maximum torque in the *XY* plane, the **STD** vehicle performs best, as the rotors are not tilted, so their full thrust range may be used to produce torque in said plane.

Considering the f_z max and the current consumption in hovering, it is expected for the **STD** and **PPNN** vehicles to behave better, as the rotor tilt in the **INW**, **SIDE** and **DUAL** vehicles give up performance in this aspect to improve the other features. The **COAX** vehicle sees its maximum vertical force severely degraded due to the loss of efficiency caused by the coaxial mounting of the rotors.

The poor performance of the **PPNN** regarding the maximum torques is caused by the asymmetry in the placement of the spinning direction of the propellers, that favours torque exerted in particular directions, but at the cost of a reduction in the overall performance.

While the vehicles present very different characteristics and performance, it is important to state that all of them may be able to fly normally under given conditions. Take for example the **STD** vehicle, which is a configuration widely used in commercial applications. To provide an estimate of the torques exerted by this vehicle during a regular flight, several experiments were performed under different conditions. Three types of flight were considered. First, for a near hovering state with mild correcting maneuvers, then, for standard maneuvering conditions, and finally for a very aggressive maneuvering situation, all of them while maintaining the vertical force equal to the weight of the vehicle. Table III presents the standard deviation of the torques exerted during each of these types of flights, discriminating between the *X* and *Y* axes and the *Z* axis, as they showed to be ten times lower in the latter. Considering the magnitude of the torques exerted in 99.7% of the cases ($\pm 3\sigma$), it is reasonable to assume that all the vehicles are able to perform satisfactorily even under aggressive maneuvering (or strong wind perturbations).

TABLE IV
CAPABILITIES OF THE VEHICLES IN A FAILURE CASE

Vehicle	q_{max} [kg m]	q_{max} XY [kg m]	f_z max [kg]	Cons. [A]
PPNN (M1 or M4)	0.00684	0.0661	0.333	31.2
PPNN (M2 or M3)	0.00195	0.0182	0.091	31.9
INW 115^o	22.3e-6	224e-6	0.531	38.3
DUAL 110^o+ 16^o	84.8e-6	150e-6	0.536	38.5

VI. ROTOR FAILURE CASE

In case of a rotor failure, it is well known that neither the **STD** nor the **SIDE** designs are able to maintain independent attitude and altitude control, while the **INW**, **DUAL** and **PPNN** are (the last one, only in cases of failures in rotors 1 to 4) [10], [14]. The **COAX** hexarotor structure has been proved to not be fault tolerant considering the characteristics stated above [15], as, in case of a failure of one rotor, the remaining rotor in the same arm has to exert a force equal to one third of the weight of the vehicle, working at its upper saturation limit. It is still feasible that a lighter vehicle, or one with oversized actuators, is fault tolerant, but this is out of the scope of this work.

In Table IV, the performance markers for each of the fault tolerant vehicles are shown for a case of failure in hovering conditions. For the **PPNN** vehicle, two cases are presented for failures in M1 or M4, and in M2 or M3 as they show very different performance, while for the **INW** and **DUAL** vehicles, all possible failures present the same characteristics due to symmetry. Comparing these values with the data shown in Table III, it can be inferred that both the **INW** and **DUAL** vehicles are extremely limited for maneuvering, and will only be capable of flying in very controlled indoor conditions, as shown in [12], [13]. The behavior of the **PPNN** vehicle will heavily depend on where the failure appears, as for a failure in M1 or M4, it may be able to fly outdoors in a mildly windy weather, with soft maneuvers, as shown in [19], while a failure in M2 or M3 will only allow for a near hovering situation.

VII. PROPOSED RECONFIGURABLE HEXAROTORS

For all the configurations presented before, in case of a failure, the maneuverability of the vehicle is severely degraded, or even null. As the maximum torques and vertical forces that can be exerted are limited by the saturation of one of the remaining functioning rotors, it can be deduced that, either one of the rotors is working too close to its operation limits, or the maneuver in the worst case demands a large variation of the force it exerts. For example, in the **STD** and the **SIDE** vehicles, when one of the rotors fails, the only feasible solution to exert zero torque and hold the hovering state (in ideal conditions, no perturbations and perfect symmetry) is that in which the opposite rotor, which generates exactly the opposite torque, exerts zero force. Then, there is a direction in which the vehicle cannot exert torque, that which would require a negative force exerted from the latter rotor, which is why the **STD** and **SIDE** vehicles are not fault tolerant.

The main idea proposed in this work is to transform the fixed hexarotor structures into reconfigurable ones in order to increase the maneuverability in case of any failure, through the addition of servomotors to tilt the rotors. The additional actuators are limited to the minimum number necessary, as they increase the weight of the vehicle, and may be an additional cause of failure. To this end, the rotors may be tilted in any direction. However, tilting them inwards or outwards results in projecting the small torque generated in the *Z* axis onto the *XY* plane, while doing it sideways allows to project the much greater torque in the *XY* plane onto the *Z* axis. Then, it is chosen to use the servomotors to tilt the rotors along the arms' axis.

For example in [20], an **INW** vehicle is modified by adding two servomotors to tilt sideways rotors 1 and 2. It is shown that adding one servomotor is not enough to increase the maneuverability in any failure case, as the failure may occur in the reconfigurable rotor, obtaining a gain the base **INW** vehicle; and that the optimal place to put the servomotors is in two adjacent rotors. In that work, an experimental proof of the increased maneuverability is also presented in case of a failure, as well as in [21] where the proposed vehicle follows a trajectory under nominal and failure circumstances. The same principle of adding two servomotors can be applied directly to the **STD** and the **SIDE** vehicle, turning them into fault tolerant systems, and to the **DUAL** vehicle to improve the performance in a failure situation.

The case of the **PPNN** vehicle is slightly different. In the other vehicles, if only one servomotor is used, a failure in the tilting motor would leave the original, poor-performance (or not fault tolerant) design. However, for the **PPNN** vehicle, there are two motors, M1 and M4 according to Table IV, that leave a vehicle with acceptable performance in case of failure. Hence, it is possible to use only one servomotor in, for example, M1, to compensate failures in M5 and M6, and to improve the performance in cases of failures in M2, M3 and M4, as will be shown below.

For the **COAX** vehicle, no significant improvement is noticed by adding either one or two servomotors, as the remaining rotor in the arm where the failure appears is still forced to work in saturation to hold the weight of the vehicle.

Consider now that, in case of a failure, rotor 1 is tilted sideways for all the considered structures except for the **COAX**. In Fig. 6, the q_{max} magnitude is shown for each of the vehicles, for every possible salvageable failure, with respect to a given side tilt of rotor 1. Similar curves are obtained by analyzing the same scenario but tilting rotor 2 instead of rotor 1. In the **STD**, **INW**, **SIDE**, and **DUAL** vehicles, servomotors have to be placed in both rotors 1 and 2 to tilt them sideways in order to have a fault tolerant vehicle with increased maneuverability. If rotor 4 fails, the pseudoinverse solution forces rotor 1 to a near-zero speed, then, modifying the orientation of rotor 1 has no significant effect on the maneuverability. However, this can still be achieved by tilting rotor 2; the same case applies if rotor 5 fails, as rotor 2 tends to shut down but rotor 1 can be tilted to compensate. For each failure, there exists an optimal point to tilt either M1 or M2, in order to obtain the maximum maneuverability for the vehicle in failure. For the **STD** and **INW** vehicles, in a case of a failure in rotor 3 or 5, it is better to use a positive tilt of rotor 1, while in case of failure of rotor 2, the only option is to use a negative tilt of rotor 1. Symmetrically, it is better to tilt rotor 2 in case of failures in rotors 1, 4 or 6. For the **SIDE** vehicle, the opposite holds, as it is shown to be better to decrease the tilting angle of rotor 1 in case of failures of rotor 2 or 6, and increase it in case of a failure in rotor 5 (as rotor 2 cannot compensate a failure in its opposite rotor); analogously, rotor 2 is tilted for failures in rotors 1, 3 or 4. In the case of the **DUAL** vehicle, rotor 1 is tilted to compensate a failure in rotors 2, 5 or 6, and rotor 2 for a failure in rotors 1, 3 or 4. By tilting rotor 1, the **PPNN** vehicle is now fault tolerant in case of failures in rotors 5 or 6, and also improves maneuverability in case of failures in rotors 2, 3 and 4, while a failure in the latter leaves the original fault tolerant design.

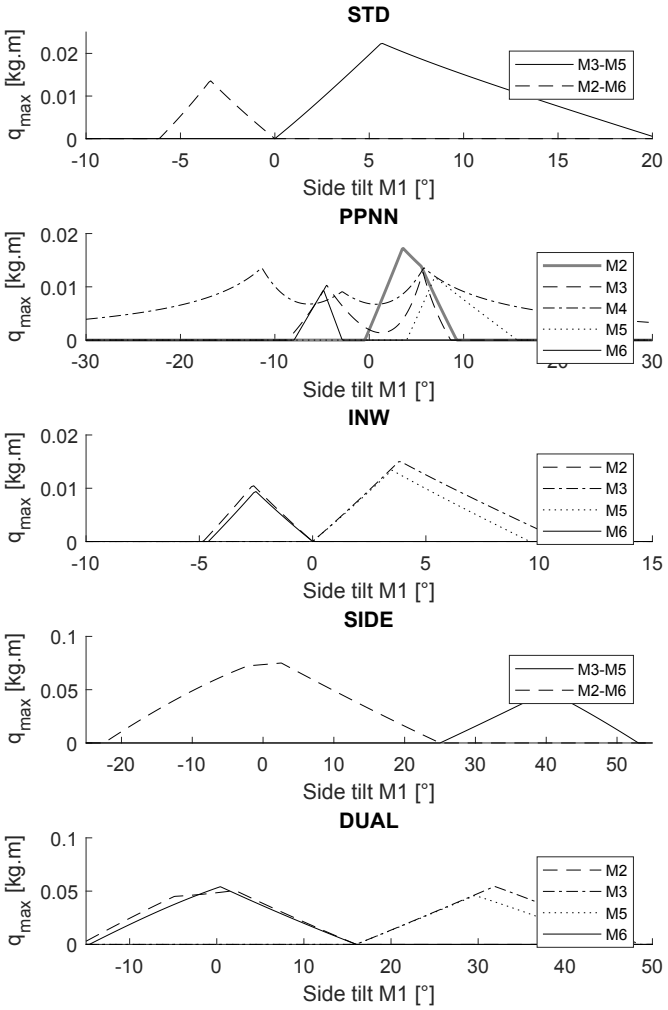

Fig. 6. q_{max} for a variable sideways tilt of rotor 1, for each of the salvageable failures, for each of the vehicles considered.

In Table V, a summary of the characteristics of the reconfigurable vehicles is shown, for the failures that result in the best and worst values of q_{max}. While, again, the vehicles that present a nominal side tilt angle different from zero are the ones that prove to be better in terms of q_{max}, in both

TABLE V
CAPABILITIES OF THE RECONFIGURABLE VEHICLES IN A FAILURE CASE

Vehicle	q_{max} [kg m]	q_{max} XY [kg m]	f_z max [kg]	Cons. [A]
Best case	—	—	—	—
STD	0.0223	0.0956	0.597	31
PPNN	0.0172	0.0790	0.469	31.2
INW	0.0150	0.0365	0.231	36.1
SIDE	0.0750	0.0755	0.493	34.6
DUAL	0.0544	0.0601	0.393	37.9
Worst case	—	—	—	—
STD	0.0136	0.0948	0.601	31
PPNN	0.0068	0.0661	0.333	31.2
INW	0.0094	0.0559	0.352	36.2
SIDE	0.0487	0.0515	0.318	38.8
DUAL	0.0458	0.0526	0.326	37.9

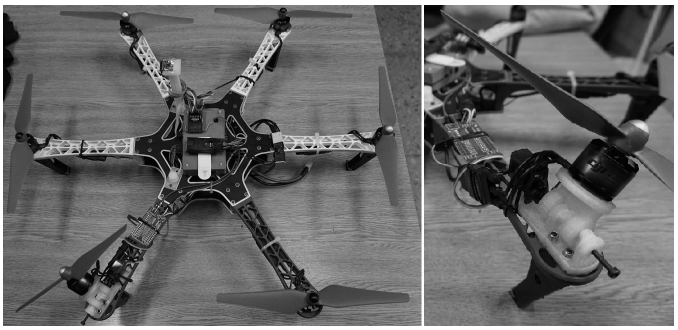

Fig. 7. Experimental model of the **STD** vehicle, with a tiltable rotor 1.

best and worst cases the **STD** vehicle appears to be better in all the other fields. Moreover, looking back at Table III, and considering again a torque range of $\pm 3\sigma$, this vehicle seems to be the most adequate to perform a flight under all conditions described, as both the q_{max} and q_{max} XY are high enough to withstand aggressive maneuvering. While the performance through this work is evaluated in terms of the feasible solutions given by the Moore-Penrose pseudoinverse of A_i, i.e., $A_i(\mathcal{U}') \subseteq \mathcal{C}$, a similar analysis was carried out considering the full torque space $\mathcal{C}$, which showed an increased value of q_{max} in all vehicles of around 10%. To obtain the performance markers for the torque space in $\mathcal{C}$ it is enough to modify Algorithm 1 as proposed in [22]. However, implementing this or other similar solutions ([14], [23]), also comes with an increased computational cost. In some cases, where the flight computer is limited in processing power, it may be not possible to run an optimization algorithm for the torque-force problem, while also considering a fault detection and identification algorithm, which is the case in the experimental test carried out in the following section.

As the **STD** vehicle shows a very good theoretical performance, it is of interest to evaluate this design in a real flight, in a situation where a failure in one of the rotors occurs.

VIII. EXPERIMENTAL CASE FOR THE **STD** VEHICLE

To provide an experimental test of the capabilities of the reconfigurable **STD** vehicle, a hexarotor was built as shown in Fig. 7 (left), with a servomotor to tilt rotor 1 as in Fig. 7 (right), with the characteristics described in Table I, except for its weight which was around $2.1\,\mathrm{kg}$. The flight computer used is a custom made board [24], that acquires sensor data and runs three PID control loops for pitch, roll and yaw angles at $200\,\mathrm{Hz}$. To detect a failure, a bank of observers based on the work in [6] is used, that allows for detection times of less than $400\,\mathrm{ms}$.

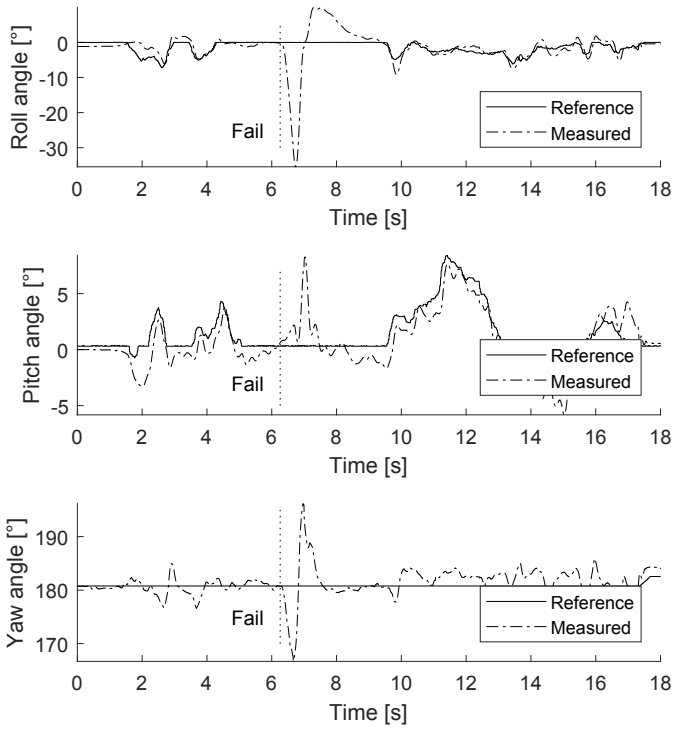

Fig. 8. Attitude of the **STD** vehicle during an outdoor flight with average winds of $30\,\mathrm{km\,h^{-1}}$, where a failure occurs in rotor 3 at t=$6.26\,\mathrm{s}$.

The vehicle was used in an outdoor environment, manually controlled by a pilot, with winds of around $30\,\mathrm{km\,h^{-1}}$. The attitude during the full flight is shown in Fig. 8, and the force exerted by each rotor in Fig. 9. The vehicle takes off, is driven to a near hovering state, and a failure is injected in rotor 3 at t=$6.26\,\mathrm{s}$. After $355\,\mathrm{ms}$, the failure is detected and the vehicle reconfigured by tilting rotor 1 from 0° to 6° according to Fig. 6 (which is done in around $13\,\mathrm{ms}$), state in which remains while performing maneuvers till it lands at t=$18\,\mathrm{s}$. The vehicle is able to follow satisfactorily the references in attitude, while the forces exerted by the rotors are well inside the operation limits, even in failure state. A full video of this particular experiment, together with several others, can be found at [25]. Another experimental proof can be found at [21] for position tracking in indoor environments in case of failure.

IX. DISCUSSION AND CONCLUSIONS

Given the fact that a minimum of 6 unidirectional actuators are needed in a multirotor vehicle in order to achieve fault tolerance in the sense of maintaining 4DOF independent control in case of a total failure of one of the rotors, this work has analyzed the maneuvering capability of six fixed-

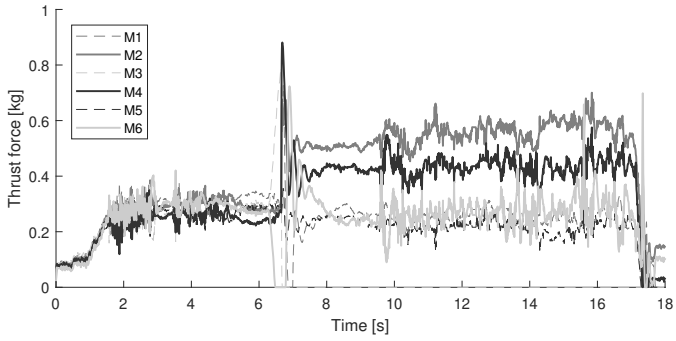

Fig. 9. Force commanded to each of the rotors of the **STD** vehicle during an outdoor flight with average winds of $30\,\mathrm{km\,h^{-1}}$, where a failure occurs in rotor 3 at t=6.26 s. The maximum force a rotor can exert is 1 kg.

structure hexarotors, with commercial characteristics, both in the nominal and in a failure case.

It was shown that all the vehicles analyzed have good maneuverability in the nominal case, and are feasible for use on real outdoors applications. However, for the vehicles which are fully fault tolerant (**INW**, **DUAL**), the maneuverability is severely degraded in case of a failure in any rotor, rendering them unusable for standard flight missions, but still flight-capable in controlled environments. For the **PPNN** vehicle, which is fault tolerant for four of the six possible failures, the maneuverability is considerably better than the previous cases, but not enough for a flight with high perturbations.

By adding servomotors to tilt one or two rotors sideways in case of a failure, the maneuverability of all the vehicles is greatly enhanced, and the **STD** and **SIDE** vehicles are converted into fault tolerant ones. As the rotors generate torque in two directions, one parallel to its axis, and other in a direction perpendicular to both its axis and its arm, and the servomotor exerts torque in the direction parallel to the arm, the latter is under very light working conditions. Also, considering all the failures are equally probable, tilting only one of the rotors in case of a failure lowers the wear of the servomotors, extending their lifespan.

ACKNOWLEDGMENT

This work has been sponsored through the University of Buenos Aires, PDE2019, and Agencia Nacional de Promoción Científica y Tecnológica, FONCYT PICT 2016-2016 (2018-2020) (Argentina). Claudio Pose would like to thank the Peruilh foundation, whose grant made this research possible.

REFERENCES

[1] M. Saied, B. Lussier, I. Fantoni, C. Francis, H. Shraim, and G. Sanahuja. Fault diagnosis and fault-tolerant control strategy for rotor failure in an octorotor. *IEEE International Conference on Robotics and Automation*, pages 5266–5271, 2015.

[2] M. Saied, B. Lussier, I. Fantoni, C. Francis, and H. Shraim. Fault tolerant control for multiple successive failures in an octorotor: Architecture and experiments. In *2015 IEEE/RSJ International Conference on Intelligent Robots and Systems (IROS)*, pages 40–45, Sep. 2015.

[3] D. Vey and J. Lunze. Structural reconfigurability analysis of multirotor UAVs after actuator failures. *54th Conference on Decision and Control*, pages 5097–5104, 2015.

[4] Duc-Tien Nguyen, David Saussie, and Lahcen Saydy. Fault-Tolerant Control of a Hexacopter UAV based on Self-Scheduled Control Allocation. In *2018 International Conference on Unmanned Aircraft Systems (ICUAS)*, pages 385–393, 2018.

[5] D. Vey, K. Schenk, and J. Lunze. Simultaneous control reconfiguration of systems with non-isolable actuator failures. In *2016 American Control Conference (ACC)*, pages 7541–7548, July 2016.

[6] D. Vey and J. Lunze. Experimental evaluation of an active fault-tolerant control scheme for multirotor UAVs. *3rd International Conference on Control and Fault-Tolerant Systems*, pages 119–126, 2016.

[7] Muhamed Kuric, Bakir Lacevic, Nedim Osmic, and Adnan Tahirovic. RLS-based fault-tolerant tracking control of multirotor aerial vehicles. In *IEEE International Conference on Advanced Intelligent Mechatronics (AIM)*, pages 1148–1153, 07 2017.

[8] G. P. Falconi, V. A. Marvakov, and F. Holzapfel. Fault tolerant control for a hexarotor system using incremental backstepping. *IEEE Conference on Control Applications (CCA)*, pages 237–242, 2016.

[9] M. W. Mueller and R. D'Andrea. Stability and control of a quadrocopter despite the complete loss of one, two, or three propellers. In *2014 IEEE International Conference on Robotics and Automation (ICRA)*, pages 45–52, May 2014.

[10] G. Michieletto, M. Ryll, and A. Franchi. Fundamental actuation properties of multirotors: Force-moment decoupling and fail-safe robustness. *IEEE Transactions on Robotics*, 34(3):702–715, June 2018.

[11] J.I. Giribet, R. S. Sanchez-Peña, and A. S. Ghersin. Analysis and design of a tilted rotor hexacopter for fault tolerance. *IEEE Transactions on Aerospace and Electronic Systems*, 52(4):1555–1567, 2016.

[12] J. I. Giribet, C. D. Pose, A. S. Ghersin, and I. Mas. Experimental validation of a fault tolerant hexacopter with tilted rotors. *International Journal of Electrical and Electronic Engineering and Telecommunications*, 7(2):1203–1218, 2018.

[13] G. Michieletto, M. Ryll, and A. Franchi. Control of statically hoverable multi-rotor aerial vehicles and application to rotor-failure robustness for hexarotors. In *2017 IEEE International Conference on Robotics and Automation (ICRA)*, pages 2747–2752, May 2017.

[14] T. Schneider. Fault-tolerant multirotor systems. *Master Thesis, Swiss Federal Institute of Technology (ETH)*, 2011.

[15] M. Achtelik, K. Doth, D. Gurdan, and J. Stumpf. *Design of a Multi Rotor MAV with regard to Efficiency, Dynamics and Redundancy*.

[16] A. Sanjuan, F. Nejjari, and R. Sarrate. Reconfigurability analysis of multirotor uavs under actuator faults. In *2019 4th Conference on Control and Fault Tolerant Systems (SysTol)*, pages 26–31, Sep. 2019.

[17] A. Merheb, H. Noura, and F. Bateman. Emergency control of ar drone quadrotor uav suffering a total loss of one rotor. *IEEE/ASME Transactions on Mechatronics*, 22(2):961–971, April 2017.

[18] Seokkwan Yoon, William M. Chan, and Thomas H. Pulliam. Computations of torque-balanced coaxial rotor flows. In *55th AIAA Aerospace Sciences Meeting*, 2017.

[19] Hussein Mazeh, Majd Saied, Hassan Shraim, and Clovis Francis. Fault-tolerant control of an hexarotor unmanned aerial vehicle applying outdoor tests and experiments. *IFAC-PapersOnLine*, 51(22):312 – 317, 2018. 12th IFAC Symposium on Robot Control SYROCO 2018.

[20] C. D. Pose, J. I. Giribet, and I. Mas. Fault tolerance analysis of a hexarotor with reconfigurable tilted rotors. In *International Conference on Robotics and Automation (ICRA)*, Paris, France, May 2020.

[21] Claudio D. Pose, Francisco Presenza, Ignacio Mas, and Juan I. Giribet. Trajectory Following with a MAV Under Rotor Fault Conditions. In P. Campoy, editor, *11^{th} International Micro Air Vehicle Competition and Conference*, number IMAV2019-7, pages 55–59, Madrid, Spain, Sep 2019.

[22] C. D. Pose, J. I. Giribet, and A. S. Ghersin. Hexacopter fault tolerant actuator allocation analysis for optimal thrust. In *2017 International Conference on Unmanned Aircraft Systems (ICUAS)*, pages 663–671, June 2017.

[23] Thomas Schneider, G. Ducard, K. Rudin, and P. Strupler. Fault-tolerant control allocation for multirotor helicopters using parametric programming. 07 2012.

[24] L. Garberoglio, M. Meraviglia, C. D. Pose, J. I. Giribet, and I. Mas. Choriboard III: A Small and Powerful Flight Controller for Autonomous Vehicles. In *2018 Argentine Conference on Automatic Control (AADECA)*, pages 1–6, Nov 2018.

[25] Fault tolerant hexacopter - Outdoor flying test. https://www.youtube.com/watch?v=9CGn-OY6JQk.

Claudio D. Pose received the Electrical Engineer degree from the University of Buenos Aires, Argentina (2014), and he is currently a Ph.D. student working on design of fault tolerant control and navigation systems for micro aerial robots in the same university. Since 2019, he is assistant professor in the Electronics Department at the School of Engineering of the University of Buenos Aires. During 2017-2018 he did an internship at the University of Applied Sciences and Arts of Italian Switzerland in the Telecom, Telemetry and High Frequency laboratory. Claudio Pose was awarded a Ph.D. scholarship from Peruilh Foundation.

Juan I. Giribet received the Electrical Engineer degree from the University of Buenos Aires, Argentina (2003), and the Ph.D. from the University of Buenos Aires (2009). He worked in the Argentine Space Agency (CONAE) and as a consultant in aerospace applications for private companies. Currently he is professor at University of Buenos Aires and researcher at Instituto Argentino de Matemática "Alberto Calderón" - CONICET. Prof. Giribet is Senior Member of the IEEE. Since 2014, he is Director of the Master's Program in Mathematical Engineering at University of Buenos Aires.

Ignacio Mas received the Electrical Engineer degree from the Universidad de Buenos Aires, Buenos Aires, Argentina, and the Ph.D. degree in Mechanical Engineering from Santa Clara University, Santa Clara, CA, USA. He was a Satellite Systems Engineer and Spacecraft Systems Designer at NASA Ames Research Center. Dr. Mas is currently an Associate Researcher at the Argentine National Scientific and Technical Research Council (CONICET) and a Professor at the University of Buenos Aires (UBA), Buenos Aires, Argentina. His research interests include multi-robot systems, coordinated navigation, and robot formation control. He is the director of LAR Lab.

LIST OF FIGURES

1083-4435 (c) 2020 IEEE. Personal use is permitted, but republication/redistribution requires IEEE permission. See http://www.ieee.org/publications_standards/publications/rights/index.html for more information.
Authorized licensed use limited to: Auckland University of Technology. Downloaded on May 24,2020 at 23:48:01 UTC from IEEE Xplore. Restrictions apply.